Decadal modulation of the relationship between tropical southern Atlantic SST and subsequent ENSO by Pacific Decadal Oscillation

AGU ADVANCING EARTH AND SPACE SCIENCES

Geophysical Research Letters

RESEARCH LETTER
10.1029/2023GL104878

Decadal Modulation of the Relationship Between Tropical Southern Atlantic SST and Subsequent ENSO by Pacific Decadal Oscillation

Shaoyu Zhang[1,2], Yimin Liu[1,2], Buwen Dong[3], and Chen Sheng[1]

[1]State Key Laboratory of Numerical Modeling for Atmospheric Sciences and Geophysical Fluid Dynamics (LASG), Institute of Atmospheric Physics, Chinese Academy of Sciences, Beijing, China, [2]College of Earth and Planetary Sciences, University of Chinese Academy of Sciences, Beijing, China, [3]Department of Meteorology, National Centre for Atmospheric Science, University of Reading, Reading, UK

Key Points:

- The relationship between tropical southern Atlantic (TSA) SST and subsequent El Niño-Southern Oscillation (ENSO) is stronger in positive Pacific Decadal Oscillation (PDO) than in negative PDO
- In positive PDO, the TSA SST anomaly easily exerts an impact on ENSO because of a weaker and more variable Walker circulation
- In positive PDO, the stronger air-sea interaction over the tropical Pacific facilitates the maintenance of local SST and wind anomalies

Supporting Information:

Supporting Information may be found in the online version of this article.

Correspondence to:

Y. M. Liu and C. Sheng,
lym@lasg.iap.ac.cn;
shengchen@lasg.iap.ac.cn

Citation:

Zhang, S., Liu, Y., Dong, B., & Sheng, C. (2023). Decadal modulation of the relationship between tropical southern Atlantic SST and subsequent ENSO by Pacific decadal oscillation. *Geophysical Research Letters*, *50*, e2023GL104878. https://doi.org/10.1029/2023GL104878

Received 12 JUN 2023
Accepted 29 SEP 2023

Abstract This study identifies the relationship between tropical southern Atlantic (TSA) sea surface temperature anomaly (SSTA) and the El Niño-Southern Oscillation (ENSO) and focuses on how the Pacific Decadal Oscillation (PDO) modulates this relationship. Results suggest a significant but non-stationary interannual TSA-ENSO relationship which undergoes a significant decadal shift. A strong TSA-ENSO relationship is observed during the positive PDO phase, while this relationship is weak during the negative PDO phase. Two processes, involving the anomalous Pacific Walker circulation (PWC) and the intensity of air-sea interactions over the Pacific, are proposed for this decadal shift. During the positive PDO phase, the weak and variable PWC and strong air-sea interaction facilitate the development of SSTA in the tropical Pacific triggered by TSA SSTA, resulting in a strong TSA-ENSO relationship and vice versa. These findings emphasize the important role of the modulation of PDO on the TSA-ENSO relationship.

Plain Language Summary The present study finds a significant TSA-ENSO relationship that anomalous warm (cold) TSA sea surface temperature (SST) in the preceding winter is closely linked to the cold (warm) ENSO in the subsequent summer and winter. However, the TSA-ENSO interannual relationship is non-stationary, which is strong during the positive PDO phase and weak during the negative PDO phase. Two processes responsible for this non-stationary relationship are proposed. During the positive PDO phase, the weak and variable PWC is more susceptible to the TSA forcing, resulting in a strong TSA-ENSO relationship. Meanwhile, the strong air-sea interaction in the tropical Pacific also facilitates the development of SSTA triggered by TSA SSTA, leading to a strong and robust TSA-ENSO relationship. During the negative PDO phase, the situations of PWC and air-sea interaction are opposite and thus lead to a weak TSA-ENSO relationship. These findings could help to improve our understanding of the decadal variability of the ENSO evolution.

1. Introduction

The El Niño–Southern Oscillation (ENSO), which arises from large-scale coupled air-sea interactions over the tropical Pacific (e.g., Bjerknes, 1969; Jin, 1997; Neelin et al., 1998; Wyrtki, 1975), is the predominant signal of seasonal-interannual variability in the global climate system (Hu et al., 2020). Given the profound climate effects of ENSO which lead to flooding, heat waves and other serious natural disasters (Hu et al., 2020) via atmospheric teleconnections (e.g., Alexander et al., 2002; Wang, 2006; Wang et al., 2000; Yang et al., 2018), the factors influencing ENSO evolution draw widespread research attention in the scientific community.

One important issue in previous studies is the interaction between ENSO and other oceans (Wang, 2019), especially the Atlantic which is the focus of this study. ENSO exerts a strong influence on tropical Atlantic variability, but it is also affected by Atlantic forcing. Previous studies have suggested a strong interaction of ENSO with sea surface temperature anomaly (SSTA) over the tropical Atlantic, including the tropical North Atlantic (e.g., Ding et al., 2012; Ham et al., 2013; Wang et al., 2017) and equatorial Atlantic (e.g., Carton & Huang, 1994; Keenlyside & Latif, 2007; Polo et al., 2015; Zebiak, 1993). During the El Niño decaying spring, a warm SSTA with broad significant positive SSTA appears over the tropical North Atlantic (Alexander & Scott, 2002; Enfield & Mayer, 1997; Klein et al., 1999; Lee et al., 2008; Wu et al., 2020; Wu & He, 2019), which in turn facilitates the development of La Niña during the subsequent boreal winter (Wang et al., 2017; Yang et al., 2018). Similarly, the

10.1029/2023GL104878

boreal summer cooling over the equatorial Atlantic could modulate the Walker circulation and enhance the development of El Niño events during the subsequent winter (Chikamoto et al., 2020; Ding et al., 2012; Keenlyside et al., 2013; Martin-Rey et al., 2015), even though the linear relationship between the equatorial Atlantic SSTA and preceding winter ENSO is insignificant (Chang et al., 2006; Lubbecke & McPhaden, 2012; Richter et al., 2013; Tokinaga et al., 2019). However, little is known about the relationship between ENSO and the tropical South Atlantic (TSA). The variation of TSA SSTA is a major rotated empirical orthogonal function mode over the tropical Atlantic (Enfield et al., 1999; Handoh, Bigg, et al., 2006, Handoh, Matthews, et al., 2006; Huang et al., 2004). Recent studies have suggested that the TSA could be a driver in climate anomalies over Eurasia and East Asia (Sheng et al., 2022; Yang et al., 2023; Zhang et al., 2022). To date, the link between TSA SSTA and subsequent ENSO remains unclear yet, especially whether the TSA SSTA in the preceding winter-spring could influence the following ENSO.

The interannual relationship associated with ENSO is usually modulated by low-frequency multidecadal variabilities. Several studies have highlighted the strong dependence of ENSO properties on the background climate state of the Pacific, which can be affected by decadal changes in tropical Pacific (Fedorov & Philander, 2000, 2001). The structure and propagation of the ENSO mode have undergone significant changes since the Pacific climate shift of the late 1970s (Fedorov & Philander, 2000; Wang & An, 2002). Despite the associated mechanisms remaining elusive, decadal changes in the background state can certainly influence ENSO properties (An & Jin, 2000; Hu & Fedorov, 2018; Kang et al., 2014; Wang & An, 2002). For instance, extratropical decadal variations can be transmitted to the tropical ocean via atmospheric bridges (Wang & An, 2002). Observational and coupled general circulation model studies have provided evidence that the intensity of the atmospheric response to ENSO depends on the state of the North Pacific Ocean, represented by the Pacific Decadal Oscillation (PDO) (Barlow et al., 2001; Bond & Harrison, 2000; Feng et al., 2014; Kwon et al., 2013; Lee et al., 2002; Liu et al., 2021; Yu & Zwiers, 2007). The PDO has been proposed to play a crucial role in affecting ENSO teleconnections. Nevertheless, whether the PDO has the potential ability to modulate the TSA-ENSO relationship remains an open question.

After identifying the TSA-ENSO relationship, the present study mainly focuses on how the PDO modulates this relationship. The rest of the paper is organized as follows. Section 2 presents the data and methodology. Section 3 presents the main results. The summary and discussion are presented in Section 4.

2. Data and Methodology

Monthly mean variables archived at the pressure level, including three-dimensional wind and sea level pressure, are obtained from ERA5 (Hersbach et al., 2020). The horizontal resolution of ERA5 data used in this study is $1° \times 1°$ (longitude × latitude). Sea surface temperature (SST) data are obtained from Hadley Center Sea Ice and SST version one on a $1° \times 1°$ resolution (Rayner et al., 2003).

Our analyses focus on 1951–2020 and anomalies for all variables are computed as the deviations from the climatological mean over this period. The linear trend at each grid point is removed from all data sets. Seasonal mean values calculated over December, January, and February, March, April, and May, and June, July, and August are used to represent the conditions of boreal winter, spring, and summer, respectively. The season with the label (−1), (0) and (+1) represents that in the previous year, present and the following year.

The normalized area-averaged SST over the region covering 0–20°S and 30°W–10°E in the Atlantic is used to define the TSA index (TSAI; Enfield et al., 1999) during the boreal winter-spring season [D(−1)JFMAM(0)]. The Niño 3.4 index is defined as the area-averaged SSTA in the region of 5°S–5°N and 170°–120°W for the summer and winter seasons [JJA(0) and D(0)JF(1)]. The 13-year centered running mean is applied to the annual averaged PDO index to extract its interdecadal variability. The PDO features two negative phases (1951–1975, 2003–2020) and one positive phase (1976–2002). All above indices can be obtained from https://psl.noaa.gov/data/climateindices/list/. The linear trends of all indices are removed. The strength of the Pacific Walker circulation (PWC) is measured by the difference between sea level pressure averaged over the eastern (5°S−5°N, 160°−80°W) and western (5°S−5°N, 80°−160°E) tropical ocean (Choi et al., 2016; Vecchi & Soden, 2007). The statistical significance of correlations, regressions or composites is assessed based on a two-tailed Student's *t*-test. The statistical significance of variance change is assessed using *F*-test.

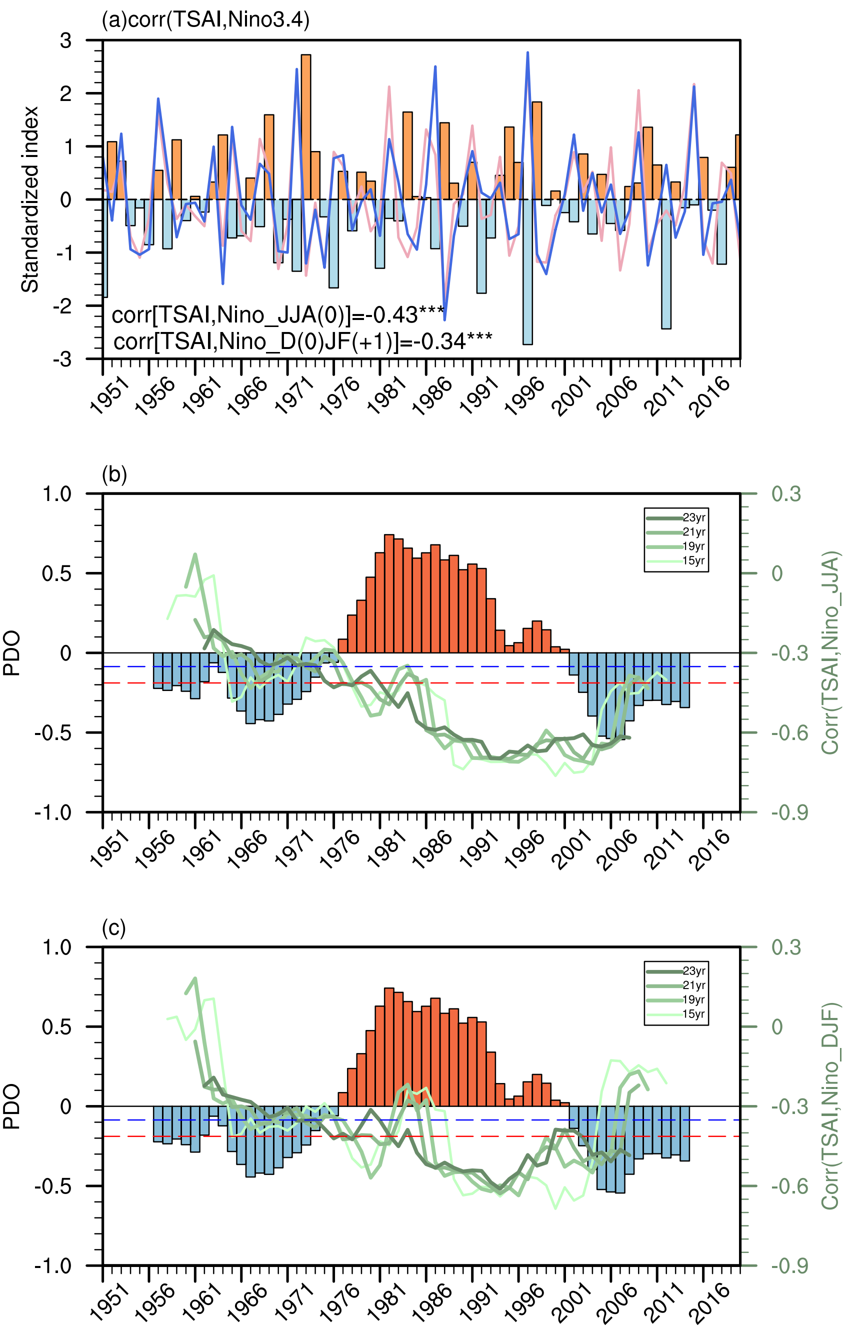

Figure 1. (a) Normalized time series of the TSA index (TSAI) (bar), Niño3.4 in JJA(0) (pink) and D(0)JF(+1) (blue). (b) Time series of the PDO (bar), the multi-year running correlation between TSAI and Niño3.4 in JJA(0) (green lines). (c) Same as (b), but for the Niño3.4 in D(0)JF(+1). The blue (red) dashed line denotes that the correlation coefficients are significant at the 0.1 (0.05) significance level based on a two-tailed Student's *t*-test. "***" indicates a significance level exceeding 0.01.

3. Results

3.1. Relationship Between TSA and ENSO and Its Decadal Shift

The time series of the TSAI and Niño3.4 are shown in Figure 1a. Interannual correlation coefficients between the winter-spring TSAI and subsequent summer and winter Niño3.4 are −0.43 and −0.34, respectively, both passing the 0.01 significance level, indicating a close interannual linkage between the preceding TSA SSTA and ENSO. This TSA-ENSO relationship suggests that La Niña events in summer to winter are typically accompanied by a

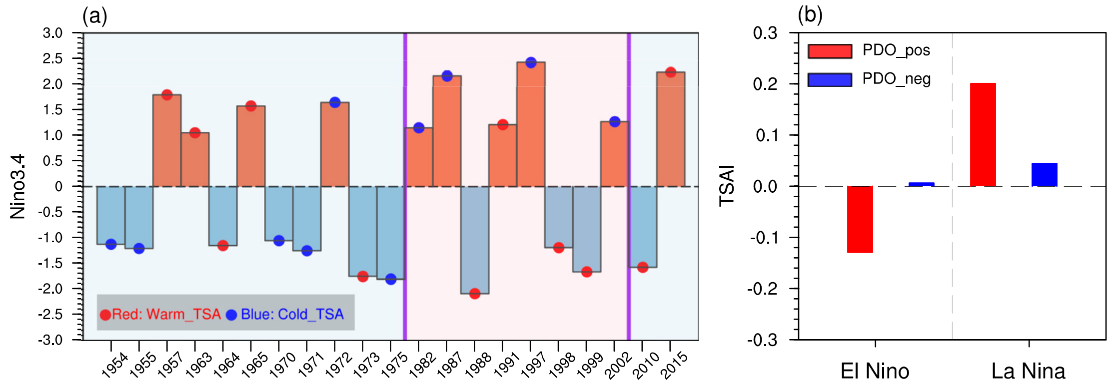

Figure 2. (a) Selected El Niño-Southern Oscillation events (bar) based on the Niño3.4 in JJA(0) and the corresponding preceding TSAI. (b) Composite TSAI in El Niño and La Niña events during the positive (red) and negative (blue) PDO phases.

preceding warm TSA SSTA, and vice versa for El Niño events. The candidate driving this relation is the anomalous Walker circulation over the equatorial Pacific (Figure S1 in Supporting Information S1). The anomalous wind embedded within the Walker circulation over the equatorial Pacific can promote the development of ENSO through positive feedback of atmosphere-ocean interactions (Bjerknes, 1969; Chikamoto et al., 2020; Ding et al., 2012). However, this TSA-ENSO relationship is nonstationary and exhibits a prominent decadal fluctuation (Figures 1b and 1c). Multi-year running correlation coefficients (Figures 1b and 1c, green solid curves) with different sliding windows show a clear nonstationary relationship that is strong in the positive PDO phase and weak in the negative PDO phase. The correlation coefficient between TSAI and Niño3.4 is −0.59 (passing the 0.01 significance level) during the PDO positive phase. However, during the PDO negative phase, the correlation coefficients are −0.25 and −0.37 which does not pass the 0.1 significance level. This nonstationary relationship is insensitive to the sliding window. We also calculate the correlation coefficients between PDO (Figures 1b and 1c; bar) and the TSA-ENSO relationship averaged in different sliding windows (Figures 1b and 1c; averaged lines), and results yield −0.54 in the following summer (Figure 1b) and −0.59 in the following winter (Figure 1c). The above results indicate that (a) there is a significant TSA-ENSO relationship that the warm (cold) TSA SSTA in the preceding winter-spring favors the development of La Niña (El Niño) in the following summer and winter and (b) this TSA-ENSO relationship is enhanced during the positive PDO phase and is weakened during the negative PDO phase.

We define an ENSO event appearing when the summer Niño 3.4 index exceeds 1 standard deviation (1 σ corresponds approximately to 0.66°C). Following this definition, 10 El Niño events and 11 La Niña events are identified. Figure 2a shows that during the positive PDO phase, both El Niño and La Niña events match well the TSA-ENSO relationship that the warm (cold) TSA corresponds to the subsequent La Niña (El Niño) event. However, the TSA-ENSO relationship is a little different in the negative PDO phase. A more visible result can be seen in Figure 2b. In the positive PDO phase (red bar in Figure 2b), El Niño (La Niña) tends to follow a cold (warm) TSA SSTA. However, this relationship breaks in the negative PDO phase (blue bar in Figure 2b). These results further confirm that the TSA-ENSO relationship is strong during the positive PDO phase and weak during the negative PDO phase.

3.2. Mechanism

3.2.1. Walker Circulation

A previous study has proposed that the atmospheric bridge rapidly conveys the effects of extratropical decadal variations to the tropics and that the Pacific decadal climate shift since the 1970s may have influenced El Niño properties by altering the background tropical winds (Wang & An, 2002). This suggests that the PDO may affect the TSA-ENSO relationship through the Walker circulation. In the following analysis, we investigate the potential mechanism by which the PDO modulates the TSA-ENSO relationship.

Figure 3 shows the seasonal evolution in spatial patterns of SSTA and 850-hPa wind associated with the TSAI during the different PDO phases. From winter to spring in all periods (first two rows in Figure 3), a significant SSTA mainly occurs over the TSA, and the SSTA over the tropical central and eastern Pacific is relatively weak. In the subsequent summer among the different PDO phases (bottom row in Figure 3), large differences in the SSTA and 850-hPa wind occur especially over the tropical Pacific, which corresponds to large differences in anomalous Walker circulation

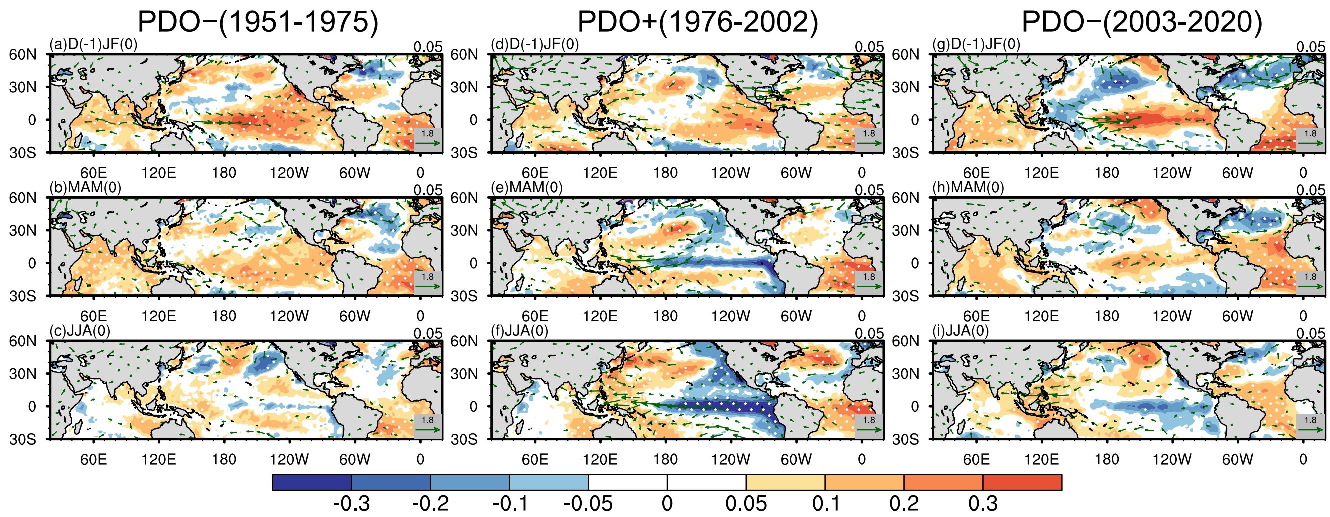

Figure 3. Spatial patterns of the regressed sea surface temperature anomaly (shading; units: K) and the regressed 850-hPa wind (vector; units: m/s) on TSAI during different PDO phases. (a), (b), and (c) represent the results averaged in D(−1)JF(0), MAM(0), and JJA(0) during the negative PDO period (1951–1975), respectively. (d)–(f) Same as (a)–(c), but for the positive PDO period (1976–2002). (g)–(i) Same as (a)–(c), but for the negative PDO period (2003–2020). The green vectors and white dots indicate the area exceeding the 0.05 significance level based on a two-tailed Student's *t*-test.

(bottom row in Figure S2 in Supporting Information S1). During the positive PDO phase, a remarkable negative SSTA and significant easterlies emerge over the tropical Pacific (Figure 3f; Figure S2f in Supporting Information S1). During the negative PDO phase, SSTA and wind anomalies over the Pacific are weak and insignificant (Figures 3c and 3i; Figures S2c and S2i in Supporting Information S1). When the impacts associated with Niño3.4 in D(−1)JF(0) are removed by linear regression, the results remain almost unchanged (figure not shown). These findings suggest that the PDO may affect the TSA-ENSO relationship through the anomalous equatorial Walker circulation, which is associated with anomalous zonal winds over the tropical Pacific and the Bjerknes feedback (Bjerknes, 1969).

Figure 4 shows the atmospheric Walker circulation associated with the PDO. Compared with the climate mean of Walker circulation (Figure 4a), the anomalous Walker circulation almost shows a reversed pattern in the positive PDO phase (Figure 4b). Specifically, there is a notable anomaly in the low-level zonal wind over the equatorial central and eastern Pacific, characterized by a persistent westerly wind anomaly (Figure 4b). This anomaly would weaken the climate mean easterly wind and weaken the climate mean SST gradient over the equatorial Pacific. To investigate further the difference in anomalous Walker circulation between the positive and negative PDO phases, we adopt the Monte Carlo bootstrapping method to estimate the probability density function of PWC strength (defined in Section 2) during both PDO phases (Figure 4c). The resampling process is executed 100,000 times. The probability density functions in the different phases of PDO are significantly separated from each other. Specifically, the anomalous PWC tends to be negative significantly in the positive PDO phase (Figure 4c), consistent with the low-level westerly wind anomalies (Figure 4b). In contrast, the PWC tends to be positive significantly in the negative PDO phase. The strength of PWC is significantly related to the PDO, with a correlation coefficient of −0.88 (Figure 4d), passing the student's *t*-test with a 0.01 significance level. Moreover, the variance of PWC during the negative PDO phase (81.93 Pa^2) is less than that during the positive phase (204.48 Pa^2). The variance difference of PWC is significant, passing the *F*-test with a 0.01 significance level, which indicates that PWC is more robust during the negative PDO phase than that in the positive PDO phase. Consequently, the TSA-ENSO connection is weak through a less variable Walker circulation during the negative PDO phase (Figure 4c). Conversely, during the positive PDO phase, the TSA-ENSO relationship is enhanced through a more variable PWC.

3.2.2. Air-Sea Interaction

We also examine the influence of low-level air–sea interactions on the TSA-ENSO relationship during different PDO phases. Similar to the linear equation for SST anomalies (Jin et al., 2006), the surface air temperature equation can be written as follows:

$$\frac{\partial T}{\partial t} = -\left(u\frac{\partial T}{\partial x} + v\frac{\partial T}{\partial y} + \omega\frac{\partial T}{\partial p}\right) + Q, \tag{1}$$

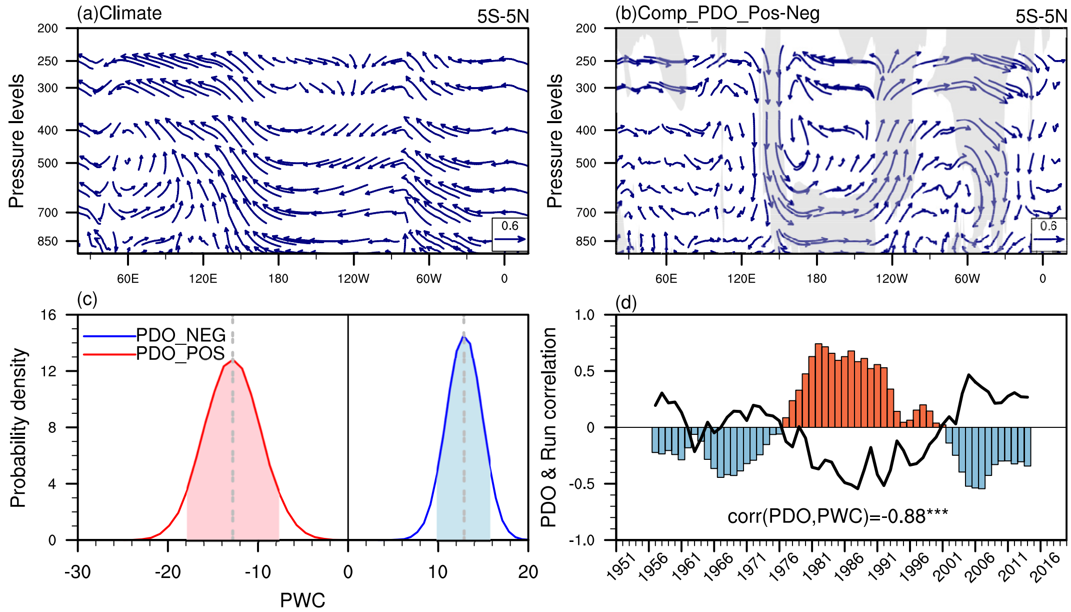

Figure 4. (a) Climatological mean of the Walker circulation (averaged from 5°S to 5°N) in MAMJJA(0) (vector: u,units: 0.1 m/s; $-10 \times \omega$, units: Pa/s). (b) Composite anomalous Walker circulation for the difference between the positive and negative PDO phases in MAMJJA(0) (vector: u, units: m/s; $-100 \times \omega$, units: Pa/s). The gray shading indicates the area where anomalies exceed the 0.1 significance level based on a two-tailed Student's *t*-test. (c) Probability density function (colored line) and average (vertical dashed line) of the Pacific Walker circulation (PWC) in MAMJJA(0) were estimated from 100,000 bootstrapped samples in the positive (red) and negative (blue) PDO phases. (d) Normalized time series of the PDO (bar) and 13-year centered running correlation between TSAI and PWC (black line). "***" indicates a significance level exceeding 0.01.

where (T, u, v, ω) represent the surface air temperature and three-dimensional wind; Q represents for net diabatic heating rate. For a zonal wind-dominated case in the equatorial central Pacific (Niño 3.4 area), Equation 1 can be simplified as:

$$\frac{\partial T}{\partial t} \approx -u\frac{\partial T}{\partial x} + Q, \tag{2}$$

Based on Jin et al. (2006) and Connolly and Lentz (2014), Q is approximately parameterized as a linear function of air-sea temperature difference (SST$-T_{2m}$). Terms in Equation 2 denote in order that the local tendency of temperature, zonal advection term showing the temperature advected by zonal wind, and the net diabatic heating rate. The composite zonal advection term in the PDO positive (negative) phase is calculated by averaging the zonal advection term during the PDO positive (negative) phase. The diagnostic results regarding the zonal advection term and the air-sea temperature difference associated with the diabatic heating term are presented in Figures 5a and 5b, respectively.

During the positive (negative) PDO phase, the impact of zonal advection is weaker (stronger) than that of the climate mean (Figure 5a), while the air-sea temperature difference is stronger (weaker) than that of the climate mean (Figure 5b). This suggests that in the positive PDO phase, the low-level atmosphere is more vulnerable to the influence of air-sea temperature difference and is more easily influenced by the SST signal rather than the atmospheric interior zonal advection, as compared to the negative PDO phase. The altered atmospheric circulation can, in turn, effectively affect the SSTA in the positive PDO phase via the Bjerknes feedback (Bjerknes, 1969) of air-sea interaction. Furthermore, following the previous study (Liu et al., 2021), we have also used the air-sea interaction index (ASI) to measure the air-sea interaction strength. The ASI is calculated as the correlation coefficient between the Niño 3.4 index and the zonal 850-hPa wind anomalies over the equatorial central Pacific (i.e., Niño 4 region). It is observed that the correlation coefficient between ASI and PDO is 0.71 (Figure 5c; passing the 0.05 significance level). The ASI is higher in the positive PDO phase than that in the negative PDO phase, which further confirms a stronger air-sea coupling in the positive PDO phase (Figure 5c). Through this strong air-sea coupling, the ENSO events triggered by TSA SSTA can develop and maintain (Figures 3e and 3f), and the resultant enhanced TSA-ENSO relationship appears in the positive PDO phase.

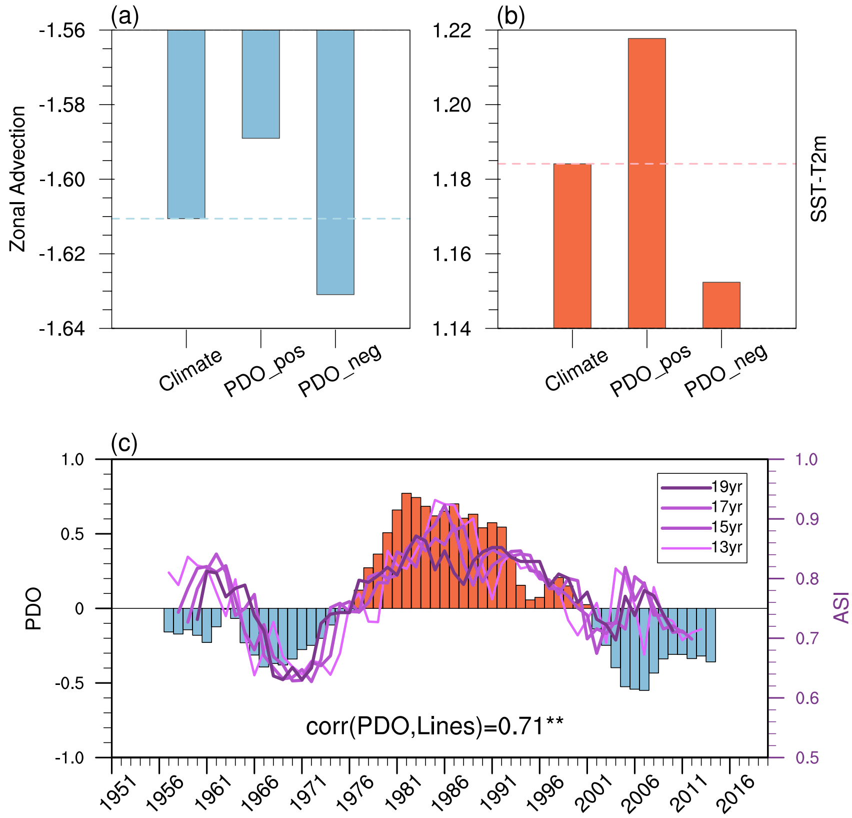

Figure 5. (a) Composite zonal advection of temperature in climate mean state, positive and negative PDO phases during MAM(0) and JJA(0) (units:10^{-6} K/s) over Niño3.4 region. (b) Same as (a), but for the difference between SST and surface air temperature (units: K). (c) Normalized time series of the PDO (bar) and multi years run of air-sea interactions index (ASI: purple lines). "**" indicates a significance level exceeding 0.05.

4. Summary and Discussion

The present study investigates the decadal modulation of the TSA-ENSO relationship by PDO and the possible mechanisms. The results are summarized as follows:

1. We identify a significant interannual TSA-ENSO relationship that the warm (cold) TSA SSTA in the preceding winter-spring is closely linked to the cold (warm) Niño3.4 in subsequent summer and winter. However, this TSA-ENSO relationship exhibits a nonstationary feature that undergoes a significant decadal shift. The TSA-ENSO relationship is strong during the positive PDO phase and weak during the negative PDO phase. During the positive PDO phase, most El Niño (La Niña) events are accompanied by a significant preceding cold (warm) TSA SSTA, whereas during the negative PDO phase, the TSA-ENSO relationship is less clear. Two reasons are proposed to elucidate this decadal shift.
2. The PWC associated with anomalous zonal winds, is proposed as a mechanism that affects the TSA-ENSO relationship. During the positive PDO phase, the weak and variable PWC is more susceptible to TSA forces, resulting in a strong TSA-ENSO relationship. In contrast, during the negative PDO phase, the PWC tends to be strong, robust, and less responsive to the forces of TSA SSTA, leading to a weak TSA-ENSO relationship.
3. The intensity of air-sea interactions in the tropical Pacific differs between the positive and negative PDO phases, significantly impacting the TSA-ENSO relationship. Specifically, during the positive PDO phase, the strong air-sea interaction facilitates the development of SST anomalies triggered by TSA SSTA, which leads to a strong and robust TSA-ENSO relationship. In contrast, the weak air-sea interaction during the negative PDO phase results in a weak TSA-ENSO relationship.

The mean state of TSA SST itself may also have an impact on the decadal shift of the TSA-ENSO relationship. We examine the TSA SST mean state and variance during the different PDO phases. In the composite analysis of PDO, changes in both mean state SST and SST variance over tropical and subtropical Atlantic are insignificant

(Figure S3 in Supporting Information S1). However, compared with the negative PDO phases (Figures 3c and 3i), the TSA SSTA is more persistent in the positive PDO phase (Figure 3f). This suggests that the influence of the persistence of TSA SSTA may also play a role in the decadal shift of the TSA-ENSO relationship and deserves further study. The processes of PWC and air-sea interaction in the tropical Pacific are two aspects behind one fact, but it is still of interest to examine their relative contributions. This work will be conducted in the future. Furthermore, future changes in anthropogenic emissions may also influence this TSA-ENSO relationship and the performance of CMIP6 models in repeating this relationship and its interdecadal change are still unknown, which also requires further study.

Conflict of Interest

The authors declare no conflicts of interest relevant to this study.

Data Availability Statement

The ERA5 reanalysis data sets are available at Hersbach et al. (2023a, 2023b). The Hadley Center SST data set is available at https://www.metoffice.gov.uk/hadobs/hadisst/data/download.html. The climate indices, including TSA, Niño 3.4 and PDO index, can be obtained from https://psl.noaa.gov/data/climateindices/list/.

Acknowledgments
This work is financially supported by the National Natural Science Foundation of China (42288101) and the Chinese Academy of Science Special Research Assistant project (2022000242).

References

Alexander, M., & Scott, J. (2002). The influence of Enso on air-sea interaction in the Atlantic. *Geophysical Research Letters*, *29*(14), 46-1–46-4. https://doi.org/10.1029/2001gl014347
Alexander, M. A., Blade, I., Newman, M., Lanzante, J. R., Lau, N. C., & Scott, J. D. (2002). The atmospheric bridge: The influence of ENSO teleconnections on air-sea interaction over the global oceans. *Journal of Climate*, *15*(16), 2205–2231. https://doi.org/10.1175/1520-0442(2002)015<2205:Tabtio>2.0.Co;2
An, S. I., & Jin, F. F. (2000). An Eigen analysis of the interdecadal changes in the structure and frequency of ENSO mode. *Geophysical Research Letters*, *27*(16), 2573–2576. https://doi.org/10.1029/1999gl011090
Barlow, M., Nigam, S., & Berbery, E. H. (2001). ENSO, Pacific decadal variability, and us summertime precipitation, drought, and stream flow. *Journal of Climate*, *14*(9), 2105–2128. https://doi.org/10.1175/1520-0442(2001)014<2105:Epdvau>2.0.Co;2
Bjerknes, J. (1969). Atmospheric teleconnections from equatorial Pacific. *Monthly Weather Review*, *97*(3), 163–172. https://doi.org/10.1175/1520-0493(1969)097<0163:Atftep>2.3.Co;2
Bond, N. A., & Harrison, D. E. (2000). The Pacific decadal oscillation, air-sea interaction and Central North Pacific winter atmospheric regimes. *Geophysical Research Letters*, *27*(5), 731–734. https://doi.org/10.1029/1999gl010847
Carton, J. A., & Huang, B. H. (1994). Warm events in the tropical Atlantic. *Journal of Physical Oceanography*, *24*(5), 888–903. https://doi.org/10.1175/1520-0485(1994)024<0888:Weitta>2.0.Co;2
Chang, P., Fang, Y., Saravanan, R., Ji, L., & Seidel, H. (2006). The cause of the fragile relationship between the Pacific El Nino and the Atlantic Nino. *Nature*, *443*(7109), 324–328. https://doi.org/10.1038/nature05053
Chikamoto, Y., Johnson, Z. F., Wang, S. Y. S., McPhaden, M. J., & Mochizuki, T. (2020). El Nino-southern oscillation evolution modulated by Atlantic forcing. *Journal of Geophysical Research-Oceans*, *125*(8). https://doi.org/10.1029/2020jc016318
Choi, J. W., Kim, I. G., Kim, J. Y., & Park, C. H. (2016). The recent strengthening of walker circulation. *Inside Solaris*, *12*(0), 96–99. https://doi.org/10.2151/sola.2016-022
Connolly, T. P., & Lentz, S. J. (2014). Interannual variability of wintertime temperature on the inner continental shelf of the middle Atlantic bight. *Journal of Geophysical Research-Oceans*, *119*(9), 6269–6285. https://doi.org/10.1002/2014jc010153
Ding, H., Keenlyside, N. S., & Latif, M. (2012). Impact of the equatorial Atlantic on the el Nino southern oscillation. *Climate Dynamics*, *38*(9–10), 1965–1972. https://doi.org/10.1007/s00382-011-1097-y
Enfield, D. B., & Mayer, D. A. (1997). Tropical Atlantic sea surface temperature variability and its relation to El Nino southern oscillation. *Journal of Geophysical Research*, *102*(C1), 929–945. https://doi.org/10.1029/96jc03296
Enfield, D. B., Mestas-Nunez, A. M., Mayer, D. A., & Cid-Serrano, L. (1999). How ubiquitous is the dipole relationship in tropical Atlantic sea surface temperatures? *Journal of Geophysical Research*, *104*(C4), 7841–7848. https://doi.org/10.1029/1998jc900109
Fedorov, A. V., & Philander, S. G. (2000). Is El Nino changing? *Science*, *288*(5473), 1997–2002. https://doi.org/10.1126/science.288.5473.1997
Fedorov, A. V., & Philander, S. G. (2001). A stability analysis of tropical ocean-atmosphere interactions: Bridging measurements and theory for El Nino. *Journal of Climate*, *14*, 3086–3101. https://doi.org/10.1175/1520-0442(2001)014<3086:Asaoto>2.0.Co;2
Feng, J., Wang, L., & Chen, W. (2014). How does the east Asian summer monsoon behave in the decaying phase of el Nino during different pdo phases? *Journal of Climate*, *27*(7), 2682–2698. https://doi.org/10.1175/jcli-d-13-00015.1
Ham, Y. G., Kug, J. S., Park, J. Y., & Jin, F. F. (2013). Sea surface temperature in the north tropical Atlantic as a trigger for El Nino/southern oscillation events. *Nature Geoscience*, *6*(2), 112–116. https://doi.org/10.1038/ngeo1686
Handoh, I. C., Bigg, G. R., Matthews, A. J., & Stevens, D. P. (2006). Interannual variability of the tropical Atlantic independent of and associated with Enso: Part II. The south tropical Atlantic. *International Journal of Climatology*, *26*(14), 1957–1976. https://doi.org/10.1002/joc.1342
Handoh, I. C., Matthews, A. J., Bigg, G. R., & Stevens, D. P. (2006). Interannual variability of the tropical Atlantic independent of and associated with ENSO: Part I. The north tropical Atlantic. *International Journal of Climatology*, *26*(14), 1937–1956. https://doi.org/10.1002/joc.1343
Hersbach, H., Bell, B., Berrisford, P., Biavati, G., Horányi, A., Muñoz Sabater, J., et al. (2023a). ERA5 monthly averaged data on pressure levels from 1940 to present [Dataset]. Copernicus Climate Change Service (C3S) Climate Data Store (CDS). https://doi.org/10.24381/cds.6860a573
Hersbach, H., Bell, B., Berrisford, P., Biavati, G., Horányi, A., Muñoz Sabater, J., et al. (2023b). ERA5 monthly averaged data on single levels from 1940 to present [Dataset]. Copernicus Climate Change Service (C3S) Climate Data Store (CDS). https://doi.org/10.24381/cds.f17050d7

Hersbach, H., Bell, B., Berrisford, P., Hirahara, S., Horanyi, A., Munoz-Sabater, J., et al. (2020). The ERA5 global reanalysis. *Quarterly Journal of the Royal Meteorological Society*, *146*(730), 1999–2049. https://doi.org/10.1002/qj.3803

Hu, S., & Fedorov, A. V. (2018). Cross-equatorial winds control El Nino diversity and change. *Nature Climate Change*, *8*(9), 798–802. https://doi.org/10.1038/s41558-018-0248-0

Hu, Z. Z., McPhaden, M. J., Kumar, A., Yu, J. Y., & Johnson, N. C. (2020). Uncoupled El Nino warming. *Geophysical Research Letters*, *47*(7). https://doi.org/10.1029/2020gl087621

Huang, B. H., Schopf, P. S., & Shukla, J. (2004). Intrinsic ocean-atmosphere variability of the tropical Atlantic ocean. *Journal of Climate*, *17*(11), 2058–2077. https://doi.org/10.1175/1520-0442(2004)017<2058:Iovott>2.0.Co;2

Jin, F. F. (1997). An equatorial ocean recharge paradigm for ENSO.1. Conceptual model. *Journal of the Atmospheric Sciences*, *54*(7), 811–829. https://doi.org/10.1175/1520-0469(1997)054<0811:Aeorpf>2.0.Co;2

Jin, F.-F., Kim, S. T., & Bejarano, L. (2006). A coupled-stability index for ENSO. *Geophysical Research Letters*, *33*(23), L23708. https://doi.org/10.1029/2006gl027221

Kang, I.-S., No, H.-h., & Kucharski, F. (2014). Enso amplitude modulation associated with the mean SST changes in the tropical central Pacific induced by Atlantic multidecadal oscillation. *Journal of Climate*, *27*(20), 7911–7920. https://doi.org/10.1175/jcli-d-14-00018.1

Keenlyside, N. S., Ding, H., & Latif, M. (2013). Potential of equatorial Atlantic variability to enhance El Nino prediction. *Geophysical Research Letters*, *40*(10), 2278–2283. https://doi.org/10.1002/grl.50362

Keenlyside, N. S., & Latif, M. (2007). Understanding equatorial Atlantic interannual variability. *Journal of Climate*, *20*(1), 131–142. https://doi.org/10.1175/jcli3992.1

Klein, S. A., Soden, B. J., & Lau, N. C. (1999). Remote sea surface temperature variations during ENSO: Evidence for a tropical atmospheric bridge. *Journal of Climate*, *12*(4), 917–932. https://doi.org/10.1175/1520-0442(1999)012<0917:Rsstvd>2.0.Co;2

Kwon, M., Yeh, S. W., Park, Y. G., & Lee, Y. K. (2013). Changes in the linear relationship of ENSO-pdo under the global warming. *International Journal of Climatology*, *33*(5), 1121–1128. https://doi.org/10.1002/joc.3497

Lee, E. J., Jhun, J. G., & Kang, I. S. (2002). The characteristic variability of boreal wintertime atmospheric circulation in El Nino events. *Journal of Climate*, *15*(8), 892–904. https://doi.org/10.1175/1520-0442(2002)015<0892:Tcvobw>2.0.Co;2

Lee, S. K., Enfield, D. B., & Wang, C. (2008). Why do some El Ninos have no impact on tropical north Atlantic SST? *Geophysical Research Letters*, *35*(16), L16705. https://doi.org/10.1029/2008gl034734

Liu, F. Y., Zhang, W. J., Jin, F. F., & Hu, S. Q. (2021). Decadal modulation of the ENSO-Indian ocean basin warming relationship during the decaying summer by the interdecadal Pacific oscillation. *Journal of Climate*, *34*(7), 2685–2699. https://doi.org/10.1175/jcli-d-20-0457.1

Lubbecke, J. F., & McPhaden, M. J. (2012). On the inconsistent relationship between Pacific and Atlantic Ninos. *Journal of Climate*, *25*(12), 4294–4303. https://doi.org/10.1175/jcli-d-11-00553.1

Martin-Rey, M., Rodriguez-Fonseca, B., & Polo, I. (2015). Atlantic opportunities for ENSO prediction. *Geophysical Research Letters*, *42*(16), 6802–6810. https://doi.org/10.1002/2015gl065062

Neelin, J. D., Battisti, D. S., Hirst, A. C., Jin, F. F., Wakata, Y., Yamagata, T., & Zebiak, S. E. (1998). Enso theory. *Journal of Geophysical Research*, *103*(C7), 14261–14290. https://doi.org/10.1029/97jc03424

Polo, I., Martin-Rey, M., Rodriguez-Fonseca, B., Kucharski, F., & Mechoso, C. R. (2015). Processes in the #pacific La Nina onset triggered by the Atlantic Nino. *Climate Dynamics*, *44*(1–2), 115–131. https://doi.org/10.1007/s00382-014-2354-7

Rayner, N. A., Parker, D. E., Horton, E. B., Folland, C. K., Alexander, L. V., Rowell, D. P., et al. (2003). Global analyses of sea surface temperature, sea ice, and night marine air temperature since the late nineteenth century. *Journal of Geophysical Research*, *108*(D14), 4407. https://doi.org/10.1029/2002jd002670

Richter, I., Behera, S. K., Masumoto, Y., Taguchi, B., Sasaki, H., & Yamagata, T. (2013). Multiple causes of interannual sea surface temperature variability in the equatorial Atlantic ocean. *Nature Geoscience*, *6*(1), 43–47. https://doi.org/10.1038/ngeo1660

Sheng, C., Wu, G. X., He, B., Liu, Y. M., & Ma, T. T. (2022). Linkage between cross-equatorial potential vorticity flux and surface air temperature over the mid-high latitudes of Eurasia during boreal spring. *Climate Dynamics*, *59*(11–12), 3247–3263. https://doi.org/10.1007/s00382-022-06259-4

Tokinaga, H., Richter, I., & Kosaka, Y. (2019). Enso influence on the Atlantic Nino, revisited: Multi-year versus single-year Enso events. *Journal of Climate*, *32*(14), 4585–4600. https://doi.org/10.1175/jcli-d-18-0683.1

Vecchi, G. A., & Soden, B. J. (2007). Global warming and the weakening of the tropical circulation. *Bulletin of the American Meteorological Society*, *88*, 1529–1530.

Wang, B., & An, S. I. (2002). A mechanism for decadal changes of Enso behavior: Roles of background wind changes. *Climate Dynamics*, *18*(6), 475–486. https://doi.org/10.1007/s00328-001-0189-5

Wang, B., Wu, R. G., & Fu, X. H. (2000). Pacific-east Asian teleconnection: How does Enso affect east Asian climate? *Journal of Climate*, *13*(9), 1517–1536. https://doi.org/10.1175/1520-0442(2000)013<1517:Peathd>2.0.Co;2

Wang, C. (2006). An overlooked feature of tropical climate: Inter-pacific-atlantic variability. *Geophysical Research Letters*, *33*(12), L12702. https://doi.org/10.1029/2006gl026324

Wang, C. Z. (2019). Three-ocean interactions and climate variability: A review and perspective. *Climate Dynamics*, *53*(7–8), 5119–5136. https://doi.org/10.1007/s00382-019-04930-x

Wang, L., Yu, J.-Y., & Paek, H. (2017). Enhanced biennial variability in the pacific due to Atlantic capacitor effect. *Nature Communications*, *8*(1), 14887. https://doi.org/10.1038/ncomms14887

Wu, R. G., & He, Z. Q. (2019). Northern tropical Atlantic warming in El Nino decaying spring: Impacts of El Nino amplitude. *Geophysical Research Letters*, *46*(23), 14072–14081. https://doi.org/10.1029/2019gl085840

Wu, R. G., Lin, M. Y., & Sun, H. M. (2020). Impacts of different types of El Nino and La Nina on northern tropical Atlantic sea surface temperature. *Climate Dynamics*, *54*(9–10), 4147–4167. https://doi.org/10.1007/s00382-020-05220-7

Wyrtki, K. (1975). El Nino—Dynamic-response of equatorial Pacific Ocean to atmospheric forcing. *Journal of Physical Oceanography*, *5*(4), 572–584. https://doi.org/10.1175/1520-0485(1975)005<0572:Entdro>2.0.Co;2

Yang, S., Li, Z. N., Yu, J. Y., Hu, X. M., Dong, W. J., & He, S. (2018). El Nino-southern oscillation and its impact in the changing climate. *National Science Review*, *5*(6), 840–857. https://doi.org/10.1093/nsr/nwy046

Yang, Y., Zhu, Z., Shen, X., Jiang, L., & Li, T. (2023). The influences of Atlantic sea surface temperature anomalies on the Enso-independent interannual variability of east Asian summer monsoon rainfall. *Journal of Climate*, *36*(2), 677–692. https://doi.org/10.1175/JCLI-D-22-0061.1

Yu, B., & Zwiers, F. W. (2007). The impact of combined Enso and pdo on the pna climate: A 1,000-year climate modeling study. *Climate Dynamics*, *29*(7–8), 837–851. https://doi.org/10.1007/s00382-007-0267-4

10.1029/2023GL104878

Zebiak, S. E. (1993). Air-sea interaction in the equatorial Atlantic region. *Journal of Climate*, *6*(8), 1567–1568. https://doi.org/10.1175/1520-0442(1993)006<1567:Aiitea>2.0.Co;2

Zhang, S. Y., Liu, Y. M., Sheng, C., & Ma, T. T. (2022). Influence of boreal spring sea surface temperature anomalies over the tropical south Atlantic on the Meiyu onset. *Climate Dynamics*, *60*(11–12), 3613–3628. https://doi.org/10.1007/s00382-022-06483-y